Journal of Industrial and Management Optimization

https://www.aimspress.com/journal/jimo

JIMO, 22(5): 2181–2207.
DOI:10.3934/jimo.2026080
Received: 29 August 2025
Revised: 10 March 2026
Accepted: 16 March 2026
Published: 01 April 2026

Research article

A correlated Heston's stochastic volatility model: A binomial tree approach

Pu-Ern Kow[1], **You-Beng Koh**[1,2,*], **Kok-Haur Ng**[1,2] **and Hailiang Yang**[3]

[1] Institute of Mathematical Sciences, Faculty of Science, Universiti Malaya, 50603 Lembah Pantai, Kuala Lumpur, Malaysia

[2] Centre of Research for Statistical Modelling and Methodology, Faculty of Science, Universiti Malaya, 50603 Lembah Pantai, Kuala Lumpur, Malaysia

[3] Department of Financial and Actuarial Mathematics, Xi'an Jiaotong-Liverpool University, Suzhou 215000, China

* **Correspondence:** Email: kohyoubeng@um.edu.my; Tel: +60-3-79674315; Fax: +60-3-79674143.

Abstract: This paper proposes a correlated binomial tree approach to model the Heston stochastic volatility process. The construction preserves the instantaneous correlation between the asset and volatility processes within a strictly recombining binomial framework. The Heston model is utilized for its ability to capture the dynamics of stochastic volatility, offering a more realistic representation of market behavior. The proposed approach improves upon existing tree-based models by incorporating the intrinsic correlation between the asset price and volatility processes, which is a key aspect of the original Heston model. Additionally, unlike Monte Carlo methods, which rely on random sampling and yield random outcomes, this approach is nonstochastic and yields convergent results with respect to the discretization of the tree. This allows for more stable and consistent parameter fitting when applied to real-world data, providing a reliable estimation of model parameters. An additional assumption that volatility remains constant during each transition is introduced, under which it is proven that the tree approach converges in distribution to the continuous Heston model under this assumption. Numerical experiments and empirical evidence from the China Securities Index 300 option market further demonstrate the robustness and practical applicability of the proposed approach, showing that it can serve as a reliable tool for both option pricing and volatility modeling in practice.

Keywords: Black-Scholes model; Heston model; binomial tree model; stochastic volatility; Cox-Ingersoll-Ross model; option pricing
Mathematics Subject Classification: 60G50, 60J65, 91-08, 91G20

1. Introduction

Options are fundamental financial instruments that offer the holder the right, but not the obligation, to buy or sell an asset at a specified price before a certain date. Option pricing is a critical area of research in financial mathematics due to its inherent complexity and the need for accurate valuation to manage risk effectively.

Black and Scholes [1] introduced the prominent Black–Scholes model to price an European option. The model uses a continuous–time framework by assuming the underlying asset follows a continuous stochastic process, which is a geometric Brownian motion. They derived a stochastic differential equation, known as the Black–Scholes equation, and further obtained the analytic solution to the Black–Scholes equation. Derman and Miller [2] stated that the current approach to model options, especially after the 1987 global stock market crash, involves considering the stochastic nature of volatility. They noted that the option market exhibits varying volatility, leading to the assumption of a stochastic volatility model, where volatility itself is a stochastic process. The local volatility model, introduced by Derman and Kani [3] and Dupire et al. [4], addresses the limitations of the Black–Scholes model by allowing the volatility to be a deterministic function of both the underlying asset price and time. However, this model still has its constraints. Heston [5] introduced the Heston model, a prominent stochastic volatility model that captures the stochastic nature of volatility more effectively, providing a comprehensive framework for pricing options under more realistic market conditions.

The discrete-time binomial tree model was first introduced in Sharpe [6], and formalized by Cox et al. [7]. Derman and Miller [2] provided a detailed explanation of how the Cox–Ross–Rubinstein (CRR) model exhibits the same first and second moments as the related geometric Brownian motion at each step. This concept highlights the equivalence in moments between the CRR model and geometric Brownian motion.

The tree approach, pioneered by the CRR model, is one of the numerical methods used to value options. This approach assumes a discrete-time jump process to model the Black–Scholes equation, which is a stochastic differential equation (SDE). By matching the local mean and variance, the CRR model converges to the said SDE as the number of steps in the CRR model increases. The CRR model, which models the constant-volatility Black–Scholes model, has constant jumps and transition probabilities at all nodes. However, this might not hold true when the volatility varies.

Pareja-Vasseur and Marín-Sánchez [8] introduced a quadrinomial tree, conceptualized as two binomial trees, to approximate stochastic volatility models. Their study primarily discusses the model proposed by Wu et al. [9], which assumes that the price process and the variance process are independent. Derman and Miller [2] also introduced the concept of modeling the Heston model using a two-dimensional binomial tree. This approach can be applied to the generalization of the quadrinomial tree framework discussed in Pareja-Vasseur and Marín-Sánchez [8] by incorporating the correlation term between the asset price process and the variance process. Additionally, Lok and Lyuu [10] introduced a tree approach for modeling local volatility models, further demonstrating the flexibility and effectiveness of tree-based methods in capturing complex volatility structures. Related tree-based constructions have also been developed for stochastic volatility and square-root processes. For example, Nawalkha and Beliaeva [11] considered efficient binomial and trinomial trees for Cox–Ingersoll–Ross (CIR) and constant elasticity of variance (CEV) type models, and Beliaeva and

Nawalkha [12] introduced an explicit tree-based implementation of the Heston model for pricing American options.

This study is motivated by the development of efficient binomial tree methods for option pricing under stochastic volatility models. Although Heston [5] derived a closed-form solution for the Heston model, it primarily focused on the pricing of European options. In practice, financial markets require the pricing of a wider range of options, including American and exotic options, which require numerical procedures under the Heston framework. The binomial tree approach offers a flexible and efficient method for modeling the behavior of the underlying asset, allowing for the pricing of various types of options. This study aims to extend the binomial tree framework to incorporate the stochastic volatility feature of the Heston model, providing a more versatile tool for option pricing in diverse market conditions. In this paper, it is assumed that the asset tree itself is a CRR tree at a certain state of volatility (see Pareja-Vasseur and Marín-Sánchez [8]). The volatility tree follows a CIR process, as assumed in the Heston model, and constructs a volatility tree under the assumptions of Nelson and Ramaswamy [13] and Lyuu [14].

The contribution of this paper is the incorporation of correlation as a constraint into the previously introduced noncorrelated binomial tree model, resulting in a deterministic algorithm for the complete Heston model, rather than a stochastic outcome from Monte Carlo simulation. Specifically, this paper adds the correlation term to the noncorrelated tree model and employs techniques from linear algebra to model the tree approach of the Heston model. The binomial tree is first constructed so that the transition structure matches the zeroth, first, and second moments of the asset and variance processes as well as the correlation term between them. To ensure feasibility of the transition probabilities, a censorship mechanism is then applied near the boundary when necessary. Numerical experiments are conducted to validate the distribution of variance using the tree approach compared to Monte Carlo simulations. The convergence of the two-dimensional binomial tree is tested under different correlation levels, including relatively high correlations, and the error analysis of the model at zero correlation with previous studies is verified. Empirical evidence from the Chinese options market is provided to solidify the model's applicability.

The remainder of the paper is organized as follows. Section 2 introduces the related models, and Section 3 discusses the tree approach to model the Heston stochastic volatility process. Numerical experiments are conducted in Section 4, and empirical evidence on the Chinese option market is given in Section 5. Lastly, Section 6 concludes the paper.

2. Binomial tree pricing model

This section introduces a binomial tree approach to model the geometric Brownian motion and CIR process. See also Fleming and Soner [15] for a detailed discussion on discrete approximations of Hamilton–Jacobi–Bellman partial differential equations. Afterward, we introduce the tree-based approach to model the Heston model. For ease of reference, some key results of the Black–Scholes option pricing model are summarized. The Black–Scholes model was introduced by Black and Scholes [1]. The Black–Scholes framework satisfies Assumption 1.

Assumption 1. *The Black–Scholes framework assumes that a financial market has at least one risky asset S_t and a risk-free asset $B(t)$ at time t. The assets satisfy the following conditions:*

1. *The risky asset S_t follows a geometric Brownian motion, which is*

$$dS_t = rS_t dt + \sigma S_t dW_t, \tag{2.1}$$

where r and σ are constants, and $\{W_t\}$ is a Wiener process.

2. *The risky asset does not pay dividends during the effective period of an option contract.*
3. *The risk-free asset pays a constant interest rate r.*
4. *There are no risk-free arbitrage opportunities in the market.*
5. *Market participants can hold any amount of risky assets and risk-free assets in either long or short positions.*
6. *There are no additional costs during transactions in the market.*
7. *The market operates continuously.*

Let $c(S, t, K, T, \sigma)$ and $p(S, t, K, T, \sigma)$ be European call and put option prices, respectively, where S, t, K, and T represent the underlying asset, current time, strike price, and expiry time, respectively. Sometimes, we use c and p to represent the European call and put options, respectively. Lemmas 1 and 2 are the results from Black and Scholes [1].

Lemma 1. *The following equation holds under Assumption 1:*

$$\frac{\partial v}{\partial t} + \frac{1}{2}\sigma^2 S^2 \frac{\partial^2 v}{\partial S^2} + rS\frac{\partial v}{\partial S} - rv = 0, \tag{2.2}$$

where $v \in \{c, p\}$.

Lemma 2. *The following equation holds under Assumption 1:*

$$c(S, t, K, T) = S\Phi(d_1) - e^{-r(T-t)}K\Phi(d_2), \tag{2.3}$$
$$p(S, t, K, T) = e^{-r(T-t)}K\Phi(-d_2) - S\Phi(-d_1), \tag{2.4}$$

where $d_1 = \dfrac{1}{\sigma\sqrt{T-t}}\left[\ln\left(\dfrac{S}{K}\right) + \left(r + \dfrac{1}{2}\sigma^2\right)(T-t)\right]$, $d_2 = d_1 - \sigma\sqrt{T-t}$, *and* $\Phi(x) = \frac{1}{\sqrt{2\pi}}\int_{-\infty}^{x} e^{-\frac{z^2}{2}} dz$.

The details of the proof can be found in Black and Scholes [1]. Let $\tilde{v}$ be market data of European option, and $v_{\mathrm{BS}}(S, t, K, T, \sigma)$ be the option pricing of the Black–Scholes formula.

Definition 1 (Implied Volatility). *The implied volatility $\tilde{\sigma}$ of an option $\tilde{v}$ satisfies*

$$v_{BS}(S, t, K, T, \tilde{\sigma}) = \tilde{v}. \tag{2.5}$$

If $\tilde{v}$ is the market price of the option, then $\tilde{\sigma}$ is the implied volatility of the market price, sometimes denoted as $\tilde{\sigma}_{mkt}$. If $\tilde{v}$ is derived from a model, then $\tilde{\sigma}$ is the implied volatility of that model.

Generally, we use the CRR model to model the asset process, which is described as geometric Brownian motion. Additionally, there are two different approaches introduced to model the CIR process.

Sharpe [6] introduced the concept of the binomial tree model for discrete-time option pricing. Subsequently, Cox et al. [7] formalized the CRR model, building upon the foundations laid by Sharpe [6]. They developed a binomial tree model that matches the first and second moments to the geometric Brownian motion.

Before introducing the binomial tree pricing model, we specify that the model requires an additional assumption beyond Assumption 1; specifically Assumption 2, as follows.

Assumption 2. *The asset price is observed discretely throughout the effective period of an option contract. We define a 'step' between two consecutive observations, during which the asset price either increases or decreases. Regardless of the starting point, two consecutive steps that first move upward and then downward, or vice versa, result in no net displacement of the asset price over the two-step horizon.*

Let $\{S_{i,j}\}$ denote the underlying price of the node at the time step i and level j, where $i = 0, 1, \ldots, n$, and for each fixed i, j takes the values

$$j = i,\ i-2,\ \ldots,\ -i.$$

Equivalently, we may write $i \in [0, n]$, $j \in [-i, i] \cap \{2\mathbb{Z} + i\}$.

The transition probability of an up move at the time step i and level j is denoted as $p_{i,j}$, where

$$p_{i,j} = \Pr\{S_{t_{i+1}} = S_{i+1,j+1} | S_{t_i} = S_{i,j}\},$$

and $i \in [0, n-1] \cap \mathbb{Z}$, $j \in [-i, i] \cap \{2\mathbb{Z} + i\}$, and let $\Delta t_i = t_{i+1} - t_i$, $i \in [0, n-1] \cap \mathbb{Z}$. The index i in $S_{i,j}$ and $p_{i,j}$ refers to the observation at time t_i. Figure 1 is a schematic representation of the binomial tree. Note that $1 - p_{i,j}$ is the transition probability of a down move at node i, j.

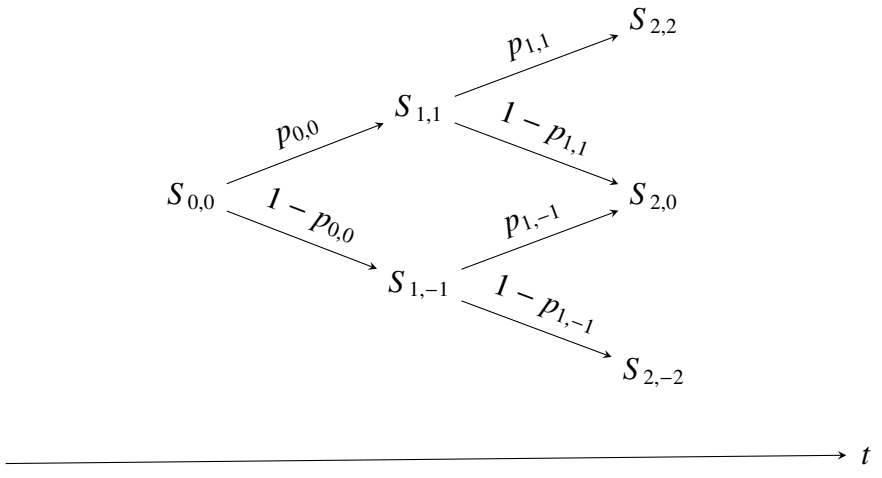

Figure 1. Schematic diagram of the two-step binomial tree model.

The binomial tree model provides a numerical result with the following steps:

1. Construct a lattice-shaped asset price tree $\{S_{i,j}\},\ i \in [0,n] \cap \mathbb{Z},\ j \in [-i,i] \cap \{2\mathbb{Z}+i\}$ along with the transition probabilities $\{p_{i,j}\},\ i \in [0,n-1] \cap \mathbb{Z},\ j \in [-i,i] \cap \{2\mathbb{Z}+i\}$ at all nodes.
2. When the option expires at the nth layer, known as at the time $t_n = T$, calculate the cash flow generated by the expired option for all possible outcomes at that layer $\{v_{n,j} = f(S_{n,j})\},\ j \in [-n,n] \cap \{2\mathbb{Z}+n\}$, where $f(x) = \max\{x-K,0\}$ for a European call option.
3. Recursively calculate the values of the preceding layer using the equation

$$v_{i,j} = e^{-r\Delta t_i}[p_{i,j}v_{i+1,j+1} + (1-p_{i,j})v_{i+1,j-1}],$$

   where $i \in [0,n-1] \cap \mathbb{Z},\ j \in [-i,i] \cap \{2\mathbb{Z}+i\}$.
4. The option pricing of the binomial tree pricing model is $v(S,t_0) = v_{0,0}$.

Note that for certain scenarios, such as model comparison, we specify that the result derived from the binomial tree pricing model is denoted as $v_{\mathrm{BT}}(S,t_0) = v_{0,0}$.

2.1. Modeling geometric Brownian motion with binomial trees

Assume that the asset price process follows the stochastic process as stated in Eq. (2.1). In the discussion of the transition from time t to $t+\Delta t$, the indices are ignored for simplicity. The CRR model assumes that the time between layers in the binomial tree is equal distanced, given by $\Delta t = T/n$. The up move magnitude u and down move magnitude d satisfy $u = d^{-1}$ (see Cox et al. [7]).

In this context, the first and second moments of the binomial tree can be matched with the corresponding moments of the Black–Scholes model. Specifically, the first moment of the binomial tree corresponds to the expected asset price, and the second moment corresponds to the asset price variance. These moments are given by the following equations:

$$\begin{aligned} pSu + (1-p)Su^{-1} &= \mathbb{E}[S_{t+\Delta t}|S_t] = Se^{r\Delta t}, \\ p[(\ln S + \ln u) - \ln S]^2 + (1-p)[(\ln S - \ln u) - \ln S]^2 &= \mathbb{E}[(\ln S_{t+\Delta t} - \ln S_t)^2|S_t] \\ &= \left[\left(r - \frac{1}{2}\sigma^2\right)\Delta t\right]^2 + \sigma^2\Delta t, \end{aligned} \tag{2.6}$$

where the left-hand sides of both equations represent the moments of the binomial tree, and the right side represents the moments of the Black–Scholes model. Considering the second moment stated in Eq. (2.6),

$$\begin{aligned} p(\ln u)^2 + (1-p)(-\ln u)^2 &= \sigma^2\Delta t + o(\Delta t), \\ (\ln u)^2 &\approx \sigma^2\Delta t. \end{aligned} \tag{2.7}$$

Solving Eqs. (2.6) and (2.7) yields

$$\begin{aligned} p &= \frac{e^{r\Delta t} - u^{-1}}{u - u^{-1}}, \\ u &\approx e^{\sigma\sqrt{\Delta t}}. \end{aligned} \tag{2.8}$$

Because Δt in the CRR model is constant, the up move magnitude u and the transition probability p, which only depend on Δt, are also constant throughout the CRR model, allowing the indices of the magnitudes and transition probabilities to be omitted in discussions of the model.

2.2. Binomial tree approach of Cox–Ingersoll–Ross model

Cox et al. [16] introduced the CIR process. The CIR process is given by

$$\mathrm{d}\nu_t = \kappa(\theta - \nu_t)\mathrm{d}t + \xi\sqrt{\nu_t}\mathrm{d}W_t, \tag{2.9}$$

where κ, θ, ξ, and ν_0 are the parameters of the model, and $\{W_t\}$ is a Wiener process.

The tree approach introduced in this section matches the first and second moments at every step, using the method introduced in [2].

Nelson and Ramaswamy [13] and Lyuu [14] introduced the tree approach to model the CIR process. See also [11], who discussed improvements on the tree framework of [13] for the CIR process. Let $\omega_t = g(\nu_t) = 2\sqrt{\nu_t}/\xi$. By Itô's lemma, we have

$$\mathrm{d}\omega_t = m(\omega_t)\mathrm{d}t + \mathrm{d}W_t, \tag{2.10}$$

where

$$m(\omega_t) = \frac{2\kappa\theta}{\xi^2\omega_t} - \frac{\kappa\omega_t}{2} - \frac{1}{2\omega_t},$$

and $\omega_0 = 2\sqrt{\nu_0}/\xi$. Let $l = \inf\{j \in \mathbb{Z} : \omega_0 + j\sqrt{\Delta t} > 0\}$ and $\{\omega_{i,j}\}$ be an n-step binomial tree of the variance process at time t_i and level j, where $i \in [0, n] \cap \mathbb{Z}$, $j \in [\max\{l, -i\}, i] \cap \{2\mathbb{Z} + i\}$. Eq. (2.10) states that ω_t has a constant variance of each step, the nodes of binomial tree $\{\omega_{i,j}\}$, to model the process ω_t are $\omega_{i,j} = \omega_0 + j\sqrt{\Delta t}$, where $i \in [0, n] \cap \mathbb{Z}$, $j \in [\max\{l, -i\}, i] \cap \{2\mathbb{Z} + i\}$ (see [14]), and Figure 2 provides an illustration of a 2-step ω_t tree.

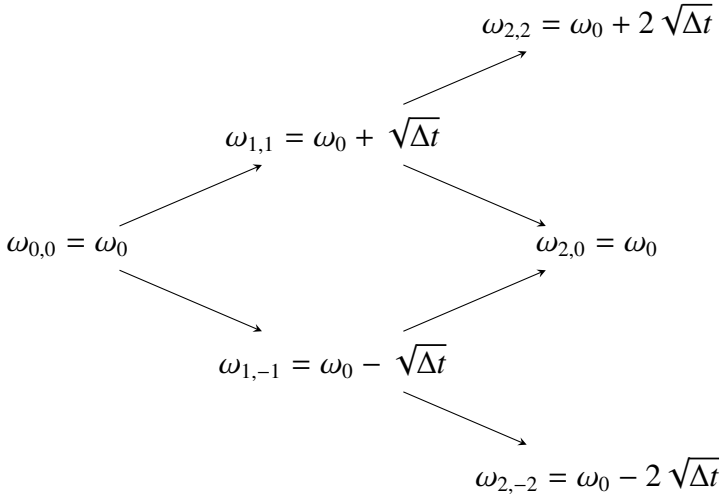

Figure 2. Schematic diagram of a 2-step ω_t tree.

Note that the binomial tree $\{\omega_{i,j}\}$ recombines because the upward and downward steps between the nodes are constant. Let $\nu_t = f(\omega_t) = (\xi^2\omega_t^2/4)\mathbb{1}_{\{\omega_t > 0\}}$, the nodes of the binomial tree $\{\nu_{i,j}\}$, model the process ν_t, given by

$$\nu_{i,j} = f(\omega_{i,j}) = \frac{\xi^2(\omega_{i,j})^2}{4}, \tag{2.11}$$

where $i \in [0, n] \cap \mathbb{Z}$, $j \in [\max\{l, -i\}, i] \cap \{2\mathbb{Z} + i\}$. Figure 3 illustrates a 2-step ν_t tree.

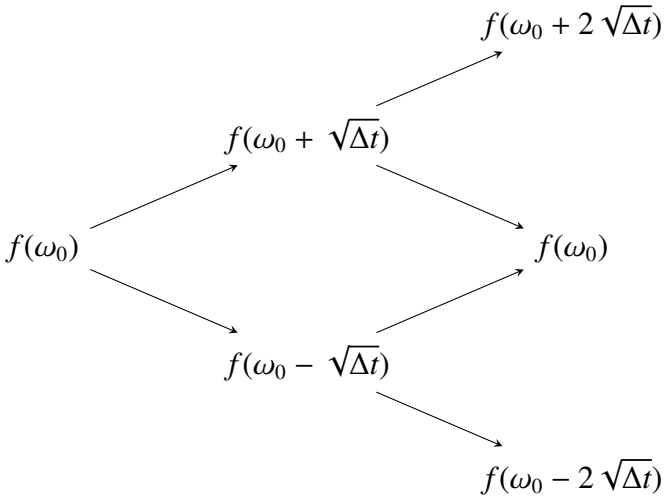

Figure 3. Schematic diagram of a 2-step ν_t tree.

The transition probability of an up move of variance at time step i and level j, $q_{i,j}$ can be approximated as

$$\begin{aligned} q_{i,j} &= \Pr\{\nu_{t_{i+1}} = \nu_{i+1,j+1} | \nu_{t_i} = \nu_{i,j}\} \\ &= \frac{\mathbb{E}[\nu_{t_{i+1}} | \nu_{t_i} = \nu_{i,j}] - \nu_{i+1,j-1}}{\nu_{i+1,j+1} - \nu_{i+1,j-1}}, \end{aligned} \tag{2.12}$$

where $\mathbb{E}[\nu_{t_{i+1}} | \nu_{t_i} = \nu_{i,j}]$ can be approximated by the Euler–Maruyama method, which is given by

$$\nu_{t+\Delta t} \approx \nu_t + \kappa(\theta - \nu_t)\Delta t + \xi\sqrt{\nu_t \Delta t} Z,$$

where $Z \sim \mathcal{N}(0, 1)$. Thus, $\mathbb{E}[\nu_{t_{i+1}} | \nu_{t_i} = \nu_{i,j}] \approx \nu_{i,j} + \kappa(\theta - \nu_{i,j})\Delta t$.

Nelson and Ramaswamy [13] introduces the censorship of the binomial tree. The modification of the up move transition probability is given by

$$\tilde{q}_{i,j} = \begin{cases} 1, & q_{i,j} > 1, \\ q_{i,j}, & q_{i,j} \in [0, 1], \\ 0, & q_{i,j} < 0. \end{cases} \tag{2.13}$$

Similarly, the down move transition probability of variance process at time step i and level j is given by $1 - \tilde{q}_{i,j}$. Note that the censorship is introduced to ensure the numerical feasibility of the binomial tree implementation under finite discretization. The censorship may introduce approximation error, particularly when ν_t approaches zero; the decay behavior of this error under time-step refinement is examined in Section 4.2. See the appendix for an asymptotic analysis of the numerical error induced by the censorship mechanism.

3. Tree approach to Heston model

The Heston model, introduced in Heston [5], is one of the stochastic volatility models. Stochastic volatility models assume that, in addition to the asset price following a geometric Brownian motion, the volatility itself is also a stochastic process. Definition 2 introduces the Heston model. Note that $\{\nu_t\}$ describes the variance process, and $\sqrt{\nu_t}$ describes the instantaneous volatility at the time t.

Definition 2 (Heston Model). *The Heston model assumes that the stock price and volatility are stochastic processes given by*

$$\begin{cases} \mathrm{d}S_t &= rS_t\mathrm{d}t + \sqrt{\nu_t}S_t\mathrm{d}W_t^S, \\ \mathrm{d}\nu_t &= \kappa(\theta-\nu_t)\mathrm{d}t + \xi\sqrt{\nu_t}\mathrm{d}W_t^\nu, \end{cases} \tag{3.1}$$

where $r, \nu_0, \theta, \rho, \kappa$, and ξ are model parameters, and $\rho\mathrm{d}t = \mathrm{d}W_t^S\,\mathrm{d}W_t^\nu$.

The binomial tree approach of Heston model is implemented under Assumption 3.

Assumption 3. *The variance is assumed to be locally constant during transitions between the nodes in the tree approach, which is given by*

$$\nu_s|\mathcal{F}_t = \nu_t, \quad \forall s \in [t, t+\Delta t),$$

where $\mathcal{F}_t$ represents the market information available at the time t.

Let $S_T^{(n)}$ denote the terminal asset price under the n-step tree model, and let $F_{n,S_T}(x)$ be its distribution. By Appendix A, $F_{n,S_T}(x)$ converges weakly to the terminal distribution $F_{S_T}(x)$ of the continuous-time Heston model. For put options, whose payoff function $\Phi(\cdot)$ is bounded and continuous, the dominated convergence theorem ensures that

$$\lim_{n\to\infty}\mathbb{E}\Big[\Phi(S_T^{(n)}) \mid \mathcal{F}_t\Big] = \mathbb{E}[\Phi(S_T) \mid \mathcal{F}_t]\,.$$

Hence, by the Feynman–Kac formula, the put option price computed from the tree model converges to the Heston option price as $n \to \infty$; the call option value is discussed separately in the numerical experiments.

Lemma 3. *The first and second moments of the asset price process and the first moment of the variance process are given by*

$$\begin{aligned} \mathbb{E}[S_{t+\Delta t} - S_t|\mathcal{F}_t] &\approx S_t r\Delta t, \\ \mathbb{E}[(S_{t+\Delta t} - S_t)^2|\mathcal{F}_t] &\approx S_t^2\int_t^{t+\Delta t}\mathbb{E}[\nu_s|\mathcal{F}_t]\mathrm{d}s, \\ \mathbb{E}[\nu_s|\mathcal{F}_t] &\approx \nu_t + \kappa(\theta-\nu_t)(s-t), \quad \forall s > t. \end{aligned} \tag{3.2}$$

Proof. By Taylor's series expansion,

$$
\begin{aligned}
S_{t+\Delta t} &= S_t \exp\left\{ \int_t^{t+\Delta t} \left(r - \frac{1}{2}\nu_s\right)\mathrm{d}s + \int_t^{t+\Delta t} \sqrt{\nu_s}\mathrm{d}W_s \right\} \\
&= S_t \Bigg\{ 1 + \left[\int_t^{t+\Delta t} \left(r - \frac{1}{2}\nu_s\right)\mathrm{d}s + \int_t^{t+\Delta t} \sqrt{\nu_s}\mathrm{d}W_s \right] \\
&\quad + \frac{1}{2}\left[\int_t^{t+\Delta t} \left(r - \frac{1}{2}\nu_s\right)\mathrm{d}s + \int_t^{t+\Delta t} \sqrt{\nu_s}\mathrm{d}W_s \right]^2 \Bigg\} + o(\Delta t) \\
&= S_t \Bigg\{ 1 + r\Delta t - \frac{1}{2}\int_t^{t+\Delta t} \nu_s \mathrm{d}s + \frac{1}{2}\left[\int_t^{t+\Delta t} \sqrt{\nu_s}\mathrm{d}W_s \right]^2 \\
&\quad + \int_t^{t+\Delta t} \sqrt{\nu_s}\mathrm{d}W_s + \frac{1}{2}\left[\int_t^{t+\Delta t} \left(r - \frac{1}{2}\nu_s\right)\mathrm{d}s \right]^2 \\
&\quad + \left(\int_t^{t+\Delta t} \left(r - \frac{1}{2}\nu_s\right)\mathrm{d}s \right)\left(\int_t^{t+\Delta t} \sqrt{\nu_s}\mathrm{d}W_s \right) \Bigg\} + o(\Delta t).
\end{aligned}
$$

Note that by Itô's isometry, $\mathbb{E}\left[\int_t^{t+\Delta t} \sqrt{\nu_s}\mathrm{d}W_s \right]^2 = \mathbb{E}\left[\int_t^{t+\Delta t} \nu_s \mathrm{d}s \right]$, and

$$
\begin{aligned}
\mathbb{E}\left[\int_t^{t+\Delta t} \sqrt{\nu_s}\mathrm{d}W_s \right] &= 0, \\
\mathbb{E}\left[\int_t^{t+\Delta t} \left(r - \frac{1}{2}\nu_s\right)\mathrm{d}s \right]^2 &= o(\Delta t), \\
\mathbb{E}\left[\left(\int_t^{t+\Delta t} \left(r - \frac{1}{2}\nu_s\right)\mathrm{d}s \right)\left(\int_t^{t+\Delta t} \sqrt{\nu_s}\mathrm{d}W_s \right) \right] &= \mathbb{E}\left[\int_t^{t+\Delta t} \left(\int_t^{t+\Delta t} \left(r - \frac{1}{2}\nu_s\right)\sqrt{\nu_u}\mathrm{d}s \right)\mathrm{d}W_u \right] \\
&= 0.
\end{aligned}
$$

Thus, the conditional expectation is given by

$$
\begin{aligned}
\mathbb{E}[S_{t+\Delta t}|\mathcal{F}_t] &\approx S_t \left\{ 1 + r\Delta t - \frac{1}{2}\mathbb{E}\left[\int_t^{t+\Delta t} \nu_s \mathrm{d}s \middle| \mathcal{F}_t \right] + \frac{1}{2}\mathbb{E}\left[\left(\int_t^{t+\Delta t} \sqrt{\nu_s}\mathrm{d}W_s \right)^2 \middle| \mathcal{F}_t \right] \right\} \\
&= S_t \left\{ 1 + r\Delta t - \frac{1}{2}\mathbb{E}\left[\int_t^{t+\Delta t} \nu_s \mathrm{d}s \middle| \mathcal{F}_t \right] + \frac{1}{2}\mathbb{E}\left[\int_t^{t+\Delta t} \nu_s \mathrm{d}s \middle| \mathcal{F}_t \right] \right\} \\
&= S_t(1 + r\Delta t) \\
&= S_t e^{r\Delta t} + o(\Delta t) \\
&\approx S_t e^{r\Delta t}.
\end{aligned}
$$

Therefore, $\mathbb{E}[S_{t+\Delta t} - S_t|\mathcal{F}_t] = S_t(e^{r\Delta t} - 1) \approx S_t r\Delta t$. Similarly, by Taylor's series expansion,

$$
\begin{aligned}
S_{t+\Delta t}^2 &= S_t^2 \exp\left\{2\int_t^{t+\Delta t}\left(r-\frac{1}{2}\nu_s\right)\mathrm{d}s + 2\int_t^{t+\Delta t}\sqrt{\nu_s}\mathrm{d}W_s\right\} \\
&= S_t^2\left\{1+2\left[\int_t^{t+\Delta t}\left(r-\frac{1}{2}\nu_s\right)\mathrm{d}s + \int_t^{t+\Delta t}\sqrt{\nu_s}\mathrm{d}W_s\right]\right. \\
&\quad \left. + \frac{1}{2}(4)\left[\int_t^{t+\Delta t}\left(r-\frac{1}{2}\nu_s\right)\mathrm{d}s + \int_t^{t+\Delta t}\sqrt{\nu_s}\mathrm{d}W_s\right]^2\right\} + o(\Delta t).
\end{aligned}
$$

By Itô's isometry, the conditional expectation is given by

$$
\begin{aligned}
\mathbb{E}[S_{t+\Delta t}^2|\mathcal{F}_t] &\approx S_t^2\left\{1+2r\Delta t - \mathbb{E}\left[\int_t^{t+\Delta t}\nu_s\mathrm{d}s\middle|\mathcal{F}_t\right] + 2\mathbb{E}\left[\int_t^{t+\Delta t}\sqrt{\nu_s}\mathrm{d}W_s\middle|\mathcal{F}_t\right]^2\right\} \\
&= S_t^2\left\{1+2r\Delta t - \mathbb{E}\left[\int_t^{t+\Delta t}\nu_s\mathrm{d}s\middle|\mathcal{F}_t\right] + 2\mathbb{E}\left[\int_t^{t+\Delta t}\nu_s\mathrm{d}s\middle|\mathcal{F}_t\right]\right\} \\
&= S_t^2\left(1+2r\Delta t + \int_t^{t+\Delta t}\mathbb{E}[\nu_s|\mathcal{F}_t]\mathrm{d}s\right),
\end{aligned}
$$

and hence

$$
\begin{aligned}
\mathbb{E}[(S_{t+\Delta t}-S_t)^2|\mathcal{F}_t] &= \mathbb{E}[S_{t+\Delta t}^2 - 2S_{t+\Delta t}S_t + S_t^2|\mathcal{F}_t] \\
&= \mathbb{E}[S_{t+\Delta t}^2|\mathcal{F}_t] - 2S_t\mathbb{E}[S_{t+\Delta t}|\mathcal{F}_t] + S_t^2 \\
&\approx S_t^2\left(1+2r\Delta t + \int_t^{t+\Delta t}\mathbb{E}[\nu_s|\mathcal{F}_t]\mathrm{d}s\right) - 2S_t[S_t(1+r\Delta t)] + S_t^2 \\
&= S_t^2\int_t^{t+\Delta t}\mathbb{E}[\nu_s|\mathcal{F}_t]\mathrm{d}s.
\end{aligned}
$$

By the Euler-Maruyama method, the CIR process is discretized as

$$
\nu_s \approx \nu_t + \kappa(\theta-\nu_t)(s-t) + \xi\sqrt{\nu_t(s-t)}Z, \quad \text{for } s>t,
$$

where $Z\sim\mathcal{N}(0,1)$. Thus,

$$
\mathbb{E}[\nu_s|\mathcal{F}_t] \approx \nu_t + \kappa(\theta-\nu_t)(s-t), \quad \text{for } s>t.
$$

□

Corollary 1. *The second moment of asset price process under Assumption 3 is given by*

$$
\mathbb{E}[(S_{t+\Delta t}-S_t)^2|\mathcal{F}_t] = S_t^2\nu_t\Delta t.
$$

Proof: By Lemma 3,

$$\begin{aligned}\mathbb{E}(S_{t+\Delta t} - S_t)^2|\mathcal{F}_t] &= S_t^2 \int_t^{t+\Delta t} \mathbb{E}[\nu_s|\mathcal{F}_t]\mathrm{d}s \\ &= S_t^2 \int_t^{t+\Delta t} \nu_t \mathrm{d}s \\ &= S_t^2 \nu_t \Delta t.\end{aligned}$$

3.1. Modeling independent Heston model with binomial trees

Pareja-Vasseur and Marín-Sánchez [8] introduced quadrinomial trees to value options in a stochastic volatility model of generalized autoregressive conditional heteroskedasticity (GARCH)-diffusion type with the assumption that the asset prices governed by the Wiener processes and volatility are independent. This section discusses a variant of the framework to approximate the Heston model. Let $H_t = (S_t, \nu_t)$ be the state of Heston model, and assume that the Wiener processes W_t^S and W_t^ν are independent. We use a two-dimensional binomial tree $\{H_{i,j,k} = (S_{i,j,k}, \nu_{i,k})\}, i \in [0, n] \cap \mathbb{Z}, j, k \in [-i, i] \cap \{2\mathbb{Z} + i\}$ to model the process H_t, where the vertical axis represents the underlying asset price, and the horizontal axis represents the variance (see Figure 4). Note that the parameters of the independent Heston model are κ, θ, ξ and ν_0.

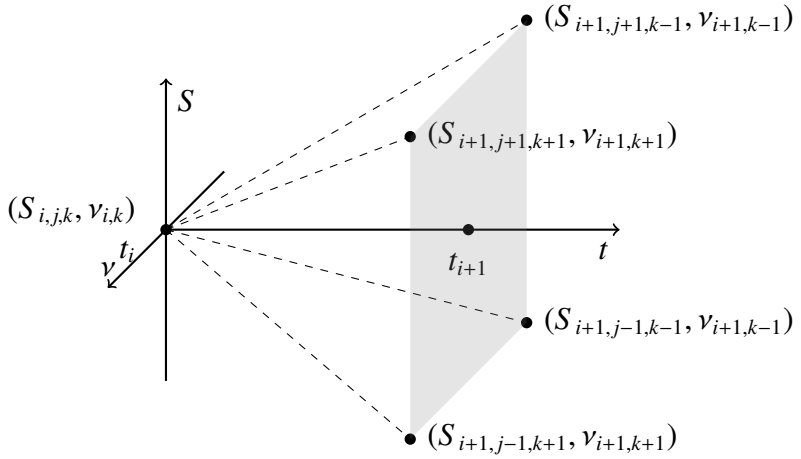

Figure 4. Schematic diagram of a one-step, two-dimensional binomial tree.

Let an up move represent an increment on asset price, a right move represent an increment on variance, and the transition probability of up and right move of $\{H_{i,j,k}\}$ at time i and levels j, k be denoted as $p_{u,r,i,j,k}$, which is given by

$$p_{u,r,i,j,k} = \Pr\{H_{t_{i+1}} = H_{i+1,j+1,k+1}|H_{t_i} = H_{i,j,k}\} = p_{i,j,k}\tilde{q}_{i,k}, \tag{3.3}$$

where $p_{i,j,k}$ is the transition probability of an increment of asset price subject to the state of variance $\nu_{i,k}$, and $\tilde{q}_{i,k}$ is the transition probability of an increment of variance. See Sections 2.1 and 2.2 for the transition probabilities of asset process and variance process.

By Corollary 1, replacing the σ with $\sqrt{\nu_{i,k}}$ in Eq. (2.8) yields

$$p_{i,j,k} = \frac{e^{r\Delta t} - e^{-\sqrt{\nu_{i,k}\Delta t}}}{e^{\sqrt{\nu_{i,k}\Delta t}} - e^{-\sqrt{\nu_{i,k}\Delta t}}}. \tag{3.4}$$

Noting that the transition of the asset price process tree, under the assumption of constant variance, allows the use of the CRR model's transition probability. Meanwhile, the transition probability of the variance tree is independent of the asset price node and can be directly obtained from the results in Section 2.2.

3.2. Modeling correlated Heston model with binomial trees

We use the same nodes introduced in Section 3.1 to model the correlated Heston model. Note that the parameters of the tree are now $\kappa, \theta, \xi, \rho$, and ν_0. Let the up, down, left, and right transition of $H_{i,j,k}$ be a one-step increment in asset price, decrement in asset price, increment in variance, and decrement in variance, respectively.

In the discussion of one-step transition, we ignore the indices i, j, and k; omit the information $\mathcal{F}_{t_i}$; and let $p_{u,r}, p_{d,r}, p_{u,l}$, and $p_{d,l}$ be the probability of up-and-right, down-and-right, up-and-left, and down-and-left transition, respectively, which is given by

$$\begin{aligned}
p_{u,r} &= \Pr\{H_{t+i+1} = H_{i+1,j+1,k+1} | H_{t_i} = H_{i,j,k}\},\\
p_{d,r} &= \Pr\{H_{t+i+1} = H_{i+1,j-1,k+1} | H_{t_i} = H_{i,j,k}\},\\
p_{u,l} &= \Pr\{H_{t+i+1} = H_{i+1,j+1,k-1} | H_{t_i} = H_{i,j,k}\},\\
p_{d,l} &= \Pr\{H_{t+i+1} = H_{i+1,j-1,k-1} | H_{t_i} = H_{i,j,k}\}.
\end{aligned}$$

Note that the transition probability differs from Eq. (3.3). Let S_u, S_d, ν_r, and ν_l be one-step increased asset price, decreased asset price, increased variance, and decreased variance, respectively; let $\mathbb{E}[\nu]$ be expected variance of the transition as given in Lemma 3; and let ν, S be variance and asset price before transition, respectively. Figure 5 illustrates the tree model with updated notations.

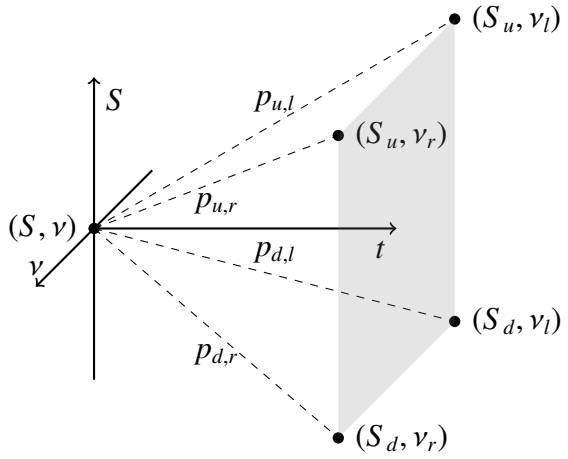

Figure 5. Schematic diagram of a one-step two-dimensional binomial tree with updated notations.

Generally, the transition probabilities sum to 1, and the first and second moments of the transition of the asset tree and the variance tree are matched, along with the correlation between the binomial tree and the Heston model. These serve as the constraints of the transition and are given as follows:

1. The transition probabilities sum to 1, given by

$$p_{u,r} + p_{d,r} + p_{u,l} + p_{d,l} = 1.$$

2. The transition probability of a one-step increment in asset is given by Eq. (3.4).

3. The transition probability of a one-step increment in variance is given by Eqs. (2.12) and (2.13).

4. Let ΔS and $\Delta\nu$ be the change of asset price and variance over the time $t_{i+1} - t_i$, respectively. The conditional covariance between them could be approximated by the Euler–Maruyama method, which is given by

$$\begin{aligned}\operatorname{cov}(\Delta S, \Delta\nu) &\approx \operatorname{cov}(S\, r\Delta t + S\,\sqrt{\nu}\Delta W^S, \kappa(\theta-\nu)\Delta t + \xi\sqrt{\nu}\Delta W^\nu)\\ &= \operatorname{cov}(S\,\sqrt{\nu}\Delta W^S, \xi\sqrt{\nu}\Delta W^\nu)\\ &= S\xi\nu\rho\Delta t.\end{aligned}$$

Matching the correlation of transition of the binomial tree and approximation above yields

$$\begin{aligned}&\operatorname{cov}(\Delta S, \Delta\nu)\\ &= \mathbb{E}[S\nu] - \mathbb{E}[S]\mathbb{E}[\nu]\\ &= [p_{u,r}S_u\nu_r + p_{u,l}S_u\nu_l + p_{d,r}S_d\nu_r + p_{d,l}S_d\nu_l] - \mathbb{E}[S]\mathbb{E}[\nu] && \text{(Tree approach)}\\ &= S\xi\nu\rho\Delta t. && \text{(Continuous process)}\end{aligned}$$

Rearranging the terms yields

$$p_{u,r}S_u\nu_r + p_{u,l}S_u\nu_l + p_{d,r}S_d\nu_r + p_{d,l}S_d\nu_l = S\xi\nu\rho\Delta t + \mathbb{E}[S]\mathbb{E}[\nu]. \tag{3.5}$$

Merging the constraints and writing them in the form of linear algebra yields the following equation:

$$\begin{bmatrix} 1 & 1 & 1 & 1\\ 1 & 0 & 1 & 0\\ 1 & 1 & 0 & 0\\ S_u\nu_r & S_d\nu_r & S_u\nu_l & S_d\nu_l \end{bmatrix}\begin{bmatrix} p_{u,r}\\ p_{d,r}\\ p_{u,l}\\ p_{d,l}\end{bmatrix} = \begin{bmatrix} 1\\ p_{i,j,k}\\ \tilde{q}_{i,k}\\ S\xi\nu\rho\Delta t + \mathbb{E}[S]\mathbb{E}[\nu]\end{bmatrix}. \tag{3.6}$$

Note that

$$\det\begin{bmatrix} 1 & 1 & 1 & 1\\ 1 & 0 & 1 & 0\\ 1 & 1 & 0 & 0\\ S_u\nu_r & S_d\nu_r & S_u\nu_l & S_d\nu_l \end{bmatrix} = (S_u - S_d)(\nu_r - \nu_l) > 0,$$

which implies the matrix is invertible, such that the solutions of the transition probability are unique and given by

$$\begin{bmatrix} p_{u,r} \\ p_{d,r} \\ p_{u,l} \\ p_{d,l} \end{bmatrix} = \begin{bmatrix} 1 & 1 & 1 & 1 \\ 1 & 0 & 1 & 0 \\ 1 & 1 & 0 & 0 \\ S_u\nu_r & S_d\nu_r & S_u\nu_l & S_d\nu_l \end{bmatrix}^{-1} \begin{bmatrix} 1 \\ p_{i,j,k} \\ \tilde{q}_{i,k} \\ S\xi\nu\rho\Delta t + \mathbb{E}[S]\mathbb{E}[\nu] \end{bmatrix}. \tag{3.7}$$

Referring to [13], we made a modification of the probability as shown in Eq. (3.8). Let $\epsilon = (\epsilon_{u,r}, \epsilon_{d,r}, \epsilon_{u,l}, \epsilon_{d,l})$ be some measure, given by

$$\epsilon_{x,y} = \begin{cases} 1, & \text{if } p_{x,y} \geq 1, \\ p_{x,y}, & \text{if } 0 < p_{x,y} < 1, \\ 0, & \text{if } p_{x,y} \leq 0, \end{cases} \tag{3.8}$$

where $(x, y) \in \{(u, r), (d, r), (u, l), (d, l)\}$.

The modified probability $\tilde{p} = (\tilde{p}_{u,r}, \tilde{p}_{d,r}, \tilde{p}_{u,l}, \tilde{p}_{d,l})$ is then given by

$$\tilde{p}_{x,y} = \frac{\epsilon_{x,y}}{\sum_{x,y} \epsilon_{x,y}}, \tag{3.9}$$

where $(x, y) \in \{(u, r), (d, r), (u, l), (d, l)\}$.

Note that the incorporation of correlation term in this section yields a different result from Section 3.1 for $\rho = 0$ at a finite step n, which implies that Eq. (3.3) does not hold under the approach introduced in this section. Section 4.3 demonstrates the numerical result of the difference between the approaches; see Appendix A.3 for proof of convergence for both approaches.

Remark 1. *Hull and White [17] analyzed the effect of correlation in their two-dimensional trinomial tree and noted that the bias induced by the correlation parameter disappears in the limit as* $\Delta t \to 0$.

The present construction removes the need to restrict the admissible range of the correlation parameter by enforcing admissibility of transition probabilities through a censoring mechanism whenever the raw moment-matching solution exits the interval $[0, 1]$.

Because the censorship modifies the transition probabilities, it introduces approximation error in the finite-step tree. However, the numerical experiments reported in Section 4.4 demonstrate convergence of the proposed method as $\Delta t \to 0$ *and stable pricing performance, including under high absolute correlation (i.e.,* $|\rho|$ *close to one).*

3.3. Calibration of parameters

Let $v_{\mathrm{HT}}(S, t, K, T, \kappa, \theta, \xi, \rho, v_0)$ represent the option pricing from tree approach of the Heston model stated in Sections 3.1 and 3.2. The implied volatility of the model is denoted as $\tilde{\sigma}_{\mathrm{HT}}$ and satisfies the equation

$$v_{\mathrm{BS}}(S, t, K, T, \tilde{\sigma}_{\mathrm{HT}}) = v_{\mathrm{HT}}(S, t, K, T, \kappa, \theta, \xi, \rho, v_0). \tag{3.10}$$

Mrázek and Pospíšil [18] and Ortiz-Ramírez et al. [19] introduced some optimizations to calibrate the parameters of the Heston model. These include

1. Minimizing the mean squared error (MSE), given by

$$\min_{\kappa,\theta,\xi,\rho\,\nu_0} \sum_{K} (\tilde{\sigma}_{\mathrm{HT}}(S,t,K,T,\kappa,\theta,\xi,\rho,\nu_0) - \tilde{\sigma}_{\mathrm{mkt}}(S,t,K,T))^2. \tag{3.11}$$

2. Minimizing the mean absolute error (MAE), given by

$$\min_{\kappa,\theta,\xi,\rho\,\nu_0} \sum_{K} |\tilde{\sigma}_{\mathrm{HT}}(S,t,K,T,\kappa,\theta,\xi,\rho,\nu_0) - \tilde{\sigma}_{\mathrm{mkt}}(S,t,K,T)|. \tag{3.12}$$

We note that [20] proposed an alternative algorithm for calibrating the Heston model, which is designed to achieve improved computational efficiency. Their approach exploits a full truncation scheme combined with an efficient optimization procedure, leading to faster convergence in the calibration process. Although the present study focuses on the numerical scheme described in Section 4, the method of [20] provides a viable and computationally efficient alternative.

4. Numerical experiments

Numerical experiments are conducted to validate the model introduced in Sections 2 and 3. The first experiment validates the tree models in modeling the CIR process by comparing the results with those from the Monte Carlo method. The second experiment involves option pricing of American options using different models. The third experiment examines the convergence of the tree models, and an error analysis between the correlated model and the relevant variant of Pareja-Vasseur and Marín-Sánchez [8] is conducted.

4.1. Validating tree method for modeling the CIR process

This section validates the accuracy of the binomial tree method in modeling the CIR process by comparing its results with those obtained using the Monte Carlo method. Consider parameters of the CIR process as $\kappa = 0.2$, $\xi = 0.05$, $\theta = 0.0625$, $\nu_0 = 0.0625$, $T = 1$, $n = 100$, and $\Delta t = T/n$. Let m be the number of stochastic processes generated and $\nu_{i,t}^{\mathrm{MC}}$ be the ith process at time t, where $i \in [1,m] \cap \mathbb{Z}$, and $t \in \{j\Delta t : j \in [1,n] \cap \mathbb{Z}\}$. The stochastic processes are generated by iterative equation, that is,

$$\nu_{i,t+\Delta t}^{\mathrm{MC}} = \max\{\nu_{i,t}^{\mathrm{MC}} + \kappa(\theta - \nu_{i,t}^{\mathrm{MC}})\Delta t + \xi\sqrt{\nu_{i,t}^{\mathrm{MC}}}\Delta W, 0\}, \tag{4.1}$$

where $\nu_{i,0}^{\mathrm{MC}} = \nu_0, \forall i \in [1,m] \cap \mathbb{Z}$, and ΔW is random number generated from the normal distribution $\mathcal{N}(0,\Delta t)$.

Let $\nu_{i,j}$ be the variance tree. Next, let G be some set of finite elements and $n(G)$ be the number of elements in the set G. The distribution function of ν_T^{MC}, derived from the Monte–Carlo method, is given by

$$\Pr\{\nu_T^{\mathrm{MC}} < x\} = \frac{n(\{i : \nu_{i,T}^{\mathrm{MC}} < x\})}{m}. \tag{4.2}$$

Figure 6 shows the comparison of terminal variance between the binomial tree approach introduced in Section 3.2 and the Monte Carlo method ($m = 10000$) in modeling the CIR process.

Note that there are discrepancies between the finite-step tree approaches and Monte Carlo simulation. As the number of time steps increases, censorship occurs on a sequence of sets whose measure converges to zero as $n \to \infty$; see Appendix A.4.

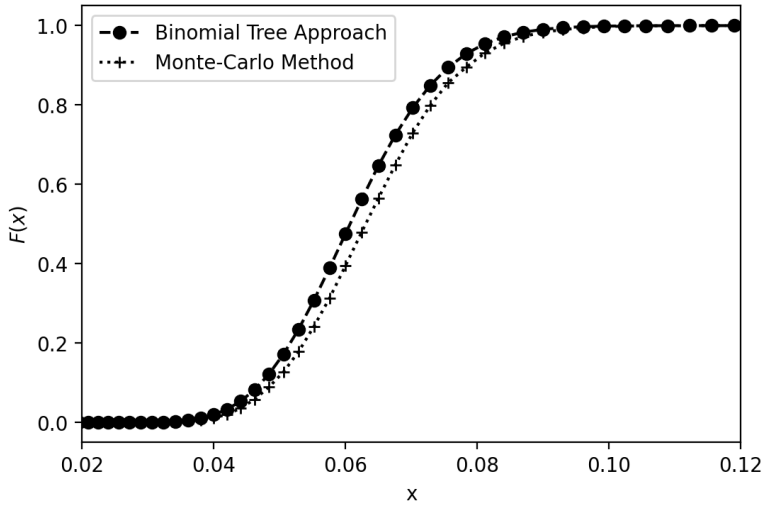

Figure 6. Distribution function of ν_T from different approaches.

4.2. Convergence of the tree model

This section studies the convergence of the two-dimensional binomial tree using the additive tree approach to model the variance tree. The parameters of the tree model are $S_0 = 100$, $K = 100$, $T = 1$, $r = 0.02$, $\theta = 0.0625$, $\nu_0 = 0.0625$, $\kappa = 0.2$, $\xi = 0.05$, and $\rho = 0$. Let a_n be the implied volatility of the n-step tree approach and $b_n = \max\{|a_k - a_n|\}$ be the maximum absolute error in implied volatility, where $k \in [n, 200] \cap \mathbb{Z}$. Figure 7a shows the maximum absolute error in implied volatility between the n-step tree and k-step tree with $k > n$. The series a_n converges if and only if $\forall \epsilon > 0$ and there exists $N = N(\epsilon)$ such that $\forall n, m > N$; we then have $|a_n - a_m| < \epsilon$. In practice, $\epsilon = 0.005$ is chosen, and a_n is considered to converge because $\forall n > 50$, $b_n < \epsilon$. Assuming a_{200} as the approximation of $\lim_{n\to\infty} a_n$, the absolute difference between a_n and a_{200} is illustrated in Figure 7b.

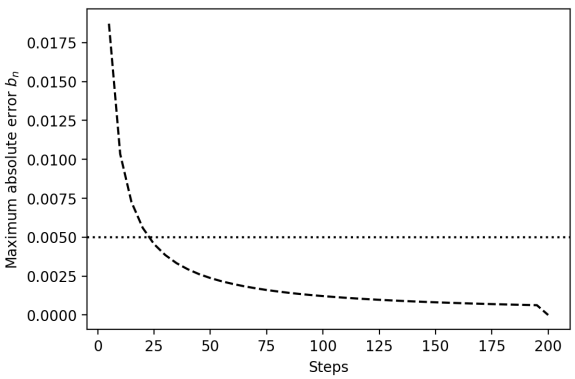

(a) Maximum absolute error in implied volatility between the n-step tree and k-step tree with $k > n$.

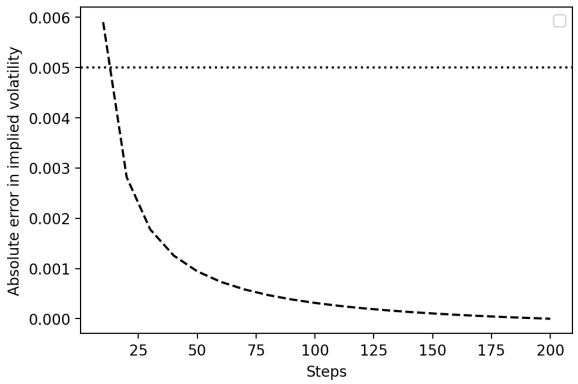

(b) Absolute error in implied volatility between the n-step tree and 200-step tree.

Figure 7. Comparison of convergence errors in implied volatility.

Figure 8 illustrates the convergence behavior of implied volatility errors with respect to the tree discretization level under different correlation settings. The comparison focuses on the decay rate of

pricing errors rather than the correlation sensitivity of the implied volatility curve itself. The results show that the magnitude of implied volatility approximation errors decreases consistently as the number of tree steps increases across different values of ρ. To provide a more detailed quantitative comparison, Table 1 reports the absolute differences in modeling errors between the cases $\rho = 0.2$ and $\rho = 0$ as well as between $\rho = -0.2$ and $\rho = 0$ at selected tree steps.

The numerical results indicate consistent error decay across different correlation settings, supporting the stability of the convergence behavior of the proposed method. Further illustrations of pricing performance under different correlation scenarios are provided in Section 4.4.

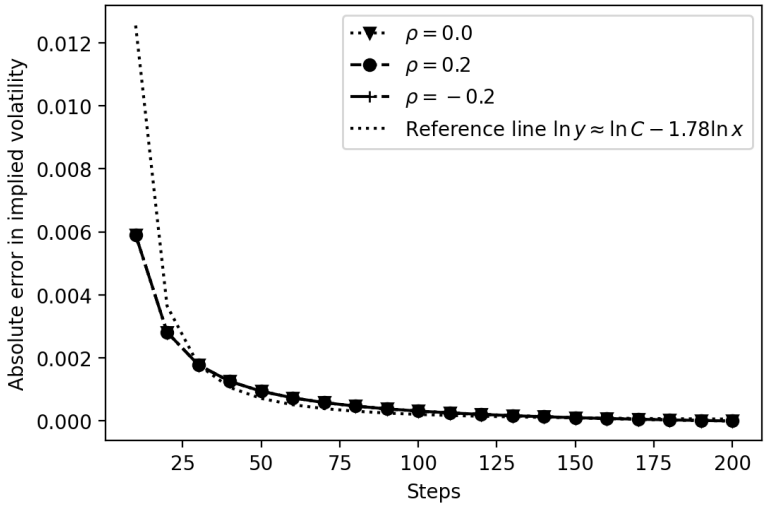

Figure 8. Comparison of convergence errors in implied volatility with different correlation.

Table 1. Decay behavior of implied volatility error differences under different correlation coefficients.

Number of tree steps	$\lvert\text{Error}_{\rho=0.2} - \text{Error}_{\rho=0}\rvert$	$\lvert\text{Error}_{\rho=-0.2} - \text{Error}_{\rho=0}\rvert$
20	1.105×10^{-6}	4.745×10^{-6}
40	3.778×10^{-7}	2.091×10^{-6}
60	2.087×10^{-7}	1.285×10^{-6}
80	1.372×10^{-7}	8.963×10^{-7}
100	9.838×10^{-8}	6.674×10^{-7}

4.3. Error analysis of the correlated model at zero-correlation and independent model

This section examines the modeling error introduced by the generalization from the independent Heston model stated in Section 3.1 to the correlated Heston model stated in Section 3.2, specifically at $\rho = 0$. The parameters of the tree model are $S_0 = 100$, $n = 50$, $T = 1$, $r = 0.02$, $\theta = 0.0625$, $v_0 = 0.0625$, $\kappa = 0.2$, and $\xi = 0.5$.

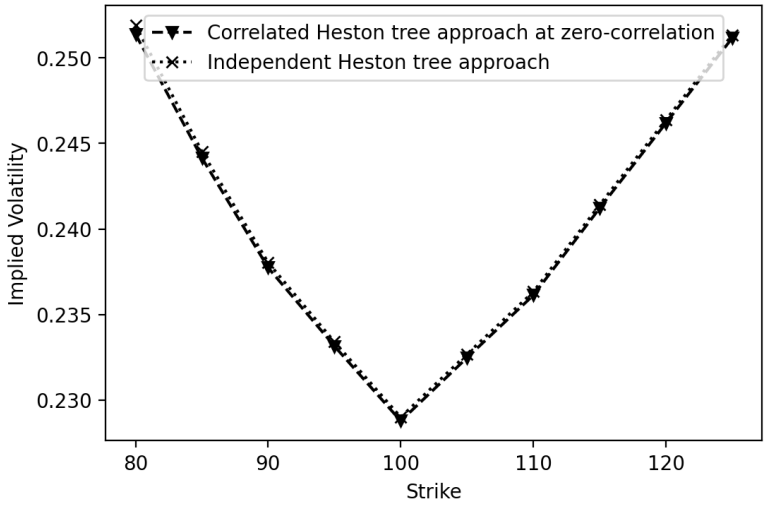

Figure 9. Comparison between the independent Heston tree approach and the correlated Heston tree approach.

Figure 9 shows the comparison of implied volatility at certain strike prices, computed using the correlated model and the corresponding variant of [8]. The proposed correlated Heston tree approach demonstrates no significant difference compared to the independent Heston tree approach under the same parameters. The generalization in Section 3.2 has an MAE of 2.664×10^{-4} in terms of implied volatility compared to the model introduced in Section 3.1. This indicates that the correlated Heston tree is a generalization of the independent Heston tree because the result of correlated Heston tree approach at zero correlation aligns closely with the independent Heston tree.

4.4. American options

This section compares American option pricing using a tree-based approach and the Monte Carlo method with the Longstaff–Schwartz algorithm (see Longstaff and Schwartz [21]). A related tree-based approach specifically designed for stochastic volatility models was also discussed in Beliaeva and Nawalkha [12], which demonstrated efficient and accurate pricing of American options under the Heston model. The parameters of the tree model are $S_0 = 100$, $n = 50$, $T = 1$, $r = 0.02$, $\theta = 0.2$, $v_0 = 0.2$, $\kappa = 0.5$, and $\xi = 0.1$. Figure 10 illustrates the option prices obtained using the Monte Carlo method when $\rho = 0$, with the 200-step tree approach serving as a reference.
The volatility paths are simulated according to Eq. (4.1), and the asset price process is given by

$$S^{\mathrm{MC}}_{i,t+\Delta t} = \max\left\{S^{\mathrm{MC}}_{i,t} + rS^{\mathrm{MC}}_{i,t}\Delta t + S^{\mathrm{MC}}_{i,t}\sqrt{v^{\mathrm{MC}}_{i,t}}\,\Delta W^S, 0\right\}, \tag{4.3}$$

where the Brownian motion W^S is correlated with the volatility process and is generated via a Cholesky decomposition. Figure 11 illustrates the convergence of American option prices with respect to the number of steps in the binomial tree for three cases, where the correlation coefficients are -0.2, 0, and 0.2, respectively. Because the pricing error curves for different correlation coefficients largely overlap, their relative differences are not visually distinguishable from the figure. To better quantify the impact of correlation, Table 2 reports the absolute differences in pricing errors between the cases $\rho = 0.2$ and $\rho = 0$ as well as between $\rho = -0.2$ and $\rho = 0$ at selected tree steps.

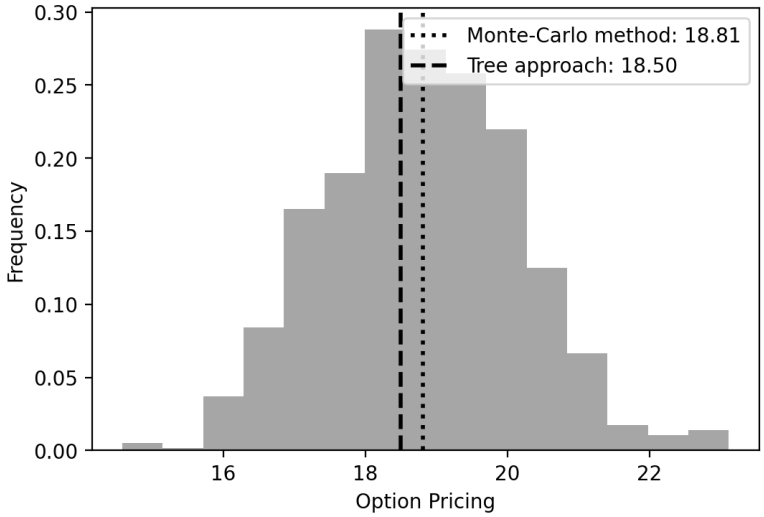

Figure 10. Comparison of American option prices computed by the Monte Carlo method and the tree-based approach.

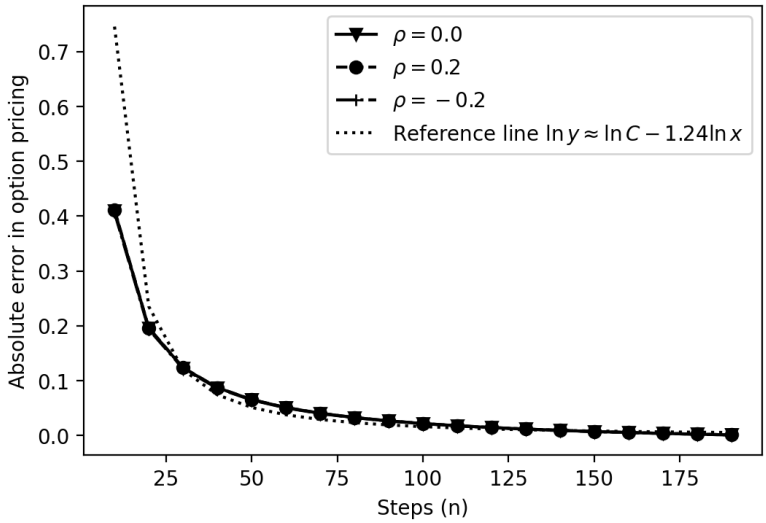

Figure 11. Convergence of pricing errors for American options.

Table 2. Error decay behavior of American option pricing approximations under different correlation coefficients.

Number of tree steps	$\lvert \text{Error}_{\rho=0.2} - \text{Error}_{\rho=0} \rvert$	$\lvert \text{Error}_{\rho=-0.2} - \text{Error}_{\rho=0} \rvert$
20	6.721×10^{-4}	2.014×10^{-3}
40	2.529×10^{-4}	9.374×10^{-4}
60	1.768×10^{-4}	5.074×10^{-4}
80	9.995×10^{-5}	3.188×10^{-4}
100	6.932×10^{-5}	2.143×10^{-4}

To further examine the robustness of the proposed methodology under stronger leverage effects,

additional experiments are conducted with $\rho = 0.7$ and $\rho = -0.7$. The corresponding convergence behavior is presented in Figure 12. As shown in Figure 12, the convergence patterns remain stable even under high absolute correlation. The pricing errors decrease consistently as the number of tree steps increases, and no numerical instability is observed. The behavior is qualitatively similar to that observed for moderate correlation levels, indicating that the proposed probability adjustment mechanism does not impair convergence under extreme ρ values.

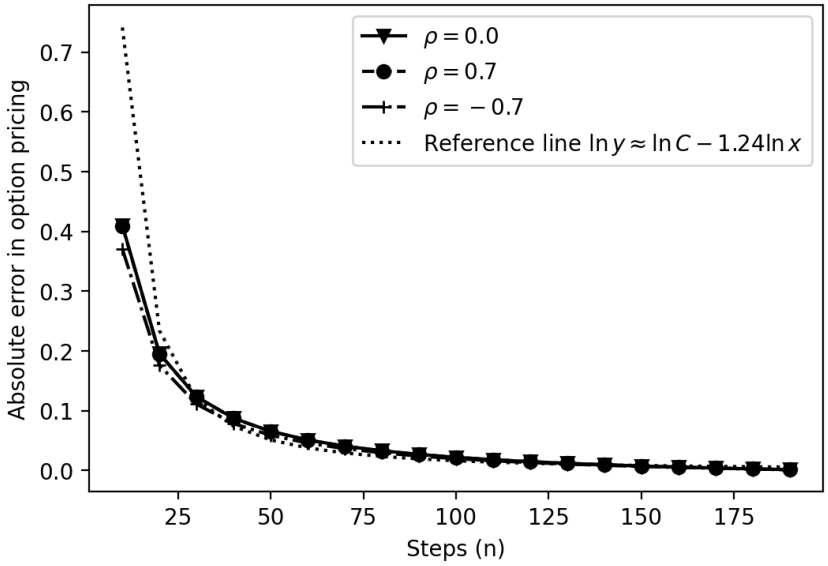

Figure 12. Convergence of pricing errors for American options under a higher leverage effect.

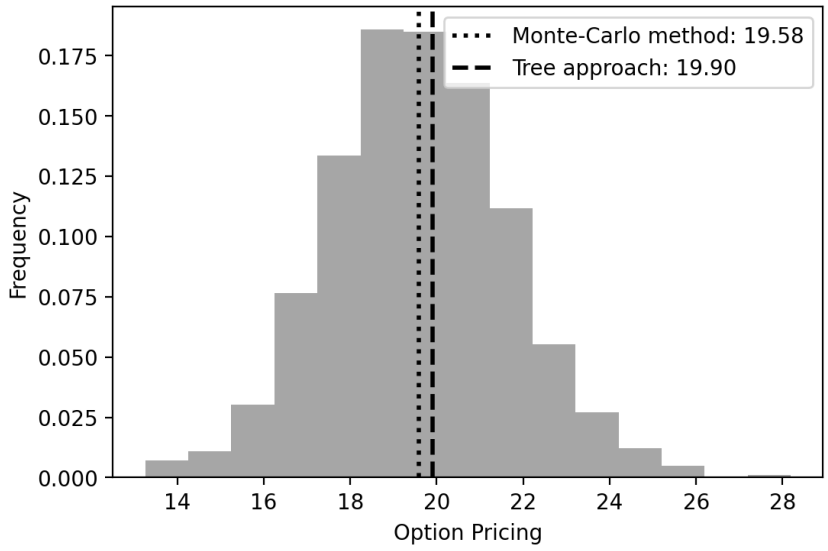

Figure 13. Comparison of American option prices computed by the Monte Carlo method and the tree-based approach under a higher leverage effect ($\rho = 0.7$).

To further validate pricing accuracy under strong positive correlation, Figure 13 compares American

option prices obtained from the proposed tree model and from the Monte Carlo benchmark in the case $\rho = 0.7$.

The Monte Carlo results are presented in the form of an empirical distribution obtained from repeated simulations, and the tree model produces a single deterministic price. As shown in Figure 13, the tree-based price lies within the central mass of the Monte Carlo distribution, and the histogram demonstrates that the two methods yield consistent valuations under $\rho = 0.7$. No systematic deviation is observed.

4.5. Discussion

The numerical experiments show that the correlated Heston tree approach is effective in modeling the Heston model. The tree approaches for modeling the variance process exhibit a distribution analogous to that obtained from the Monte Carlo method. Given the flexibility to choose the time of observation for the distribution, we can validate the tree method for modeling the variance process.

By combining the tree approach for the variance process and the CRR model for the asset process, we are able to price options. The focus is on discussing implied volatility rather than option pricing because implied volatility may more clearly reflect the effectiveness of the model, especially in pricing out-of-the-money options.

The model introduced in Section 3.2 extends the quadrinomial tree method introduced in Pareja-Vasseur and Marín-Sánchez [8] by incorporating the correlation between the asset process and the variance process. The error between the zero-correlated model and the independent model is discussed in Section 4.3. Section 4.4 shows the convergence of the tree approach in pricing American options. The convergence behavior is presented for different correlations, demonstrating the convergence under different correlations of the tree method.

5. Empirical evidence

An empirical example is provided with the contract "IO2406-C-Strike", where the underlying asset of the contract is the Chinese Security Index 300 (CSI300). The "IO2406-C-Strike" refers to call options that expire on the third Friday of June 2024 at a certain strike price. The option and government bond data are open-sourced and can be accessed for free from the official websites of the China Financial Futures Exchange (CFFEX) and ChinaBond, respectively.

The date for calibrating parameters is January 3, 2024. The parameters are $S_0 = 3378.30$, $T = 0.46$, and $r = 0.021$. The data is available at strike prices from 2900 to 4500, at an interval of 100. The steps in Heston's tree model are set to $n = 50$, and the parameters are calibrated using the 10 highest volume option contracts. The strike prices of these contracts are $\{3400, 3500, 3600, 3700, 3800, 4000, 4100, 4200, 4400, 4500\}$. The calibrated parameters obtained from minimizing the mean absolute error (see Eq. (3.12)) of the independent Heston model and correlated Heston model are shown in Table 3.

Figure 14 shows the implied volatility of the market data and the models, with model parameters listed in Table 3. Table 4 shows the MAE and MSE of both models. The empirical results demonstrate that the correlated Heston model achieves lower MAE and MSE than the independent approach, indicating improved accuracy and effectiveness in modeling the underlying processes. The calibrated negative correlation between returns and volatility reflects the leverage effect, a well-documented market phenomenon (Christie [22]). This empirically observed relationship

demonstrates that incorporating the correlation term ρ addresses a key limitation of the independence assumption between the Wiener processes W_t^S and W_t^ν.

Figure 15 illustrates the implied volatility curves calibrated using Eq. (3.12) for call options with different maturities. The corresponding contract codes are 'IO2401-C-Strike', 'IO2402-C-Strike', 'IO2403-C-Strike', 'IO2409-C-Strike', and 'IO2412-C-Strike'. Table 5 reports the MAE of the calibrated curves.

Table 3. Calibrated parameters of the independent Heston tree and correlated Heston tree.

Parameter	Independent Heston tree	Correlated Heston tree
θ	0.0675	0.0685
κ	0.2351	0.2368
ξ	0.3352	0.3383
ν_0	0.0253	0.0256
ρ	N/A	-0.0319

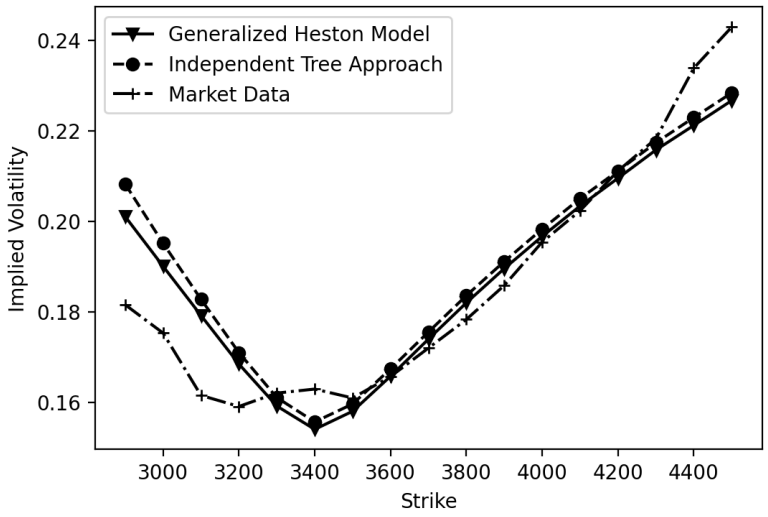

Figure 14. Implied volatility of CSI300 Index call options on January 3, 2024.

Table 4. Comparison of the mean absolute error and mean squared error of two models.

Loss function	Independent Heston tree	Correlated Heston tree
MAE	8.058×10^{-3}	7.104×10^{-3}
MSE	1.278×10^{-4}	9.183×10^{-5}

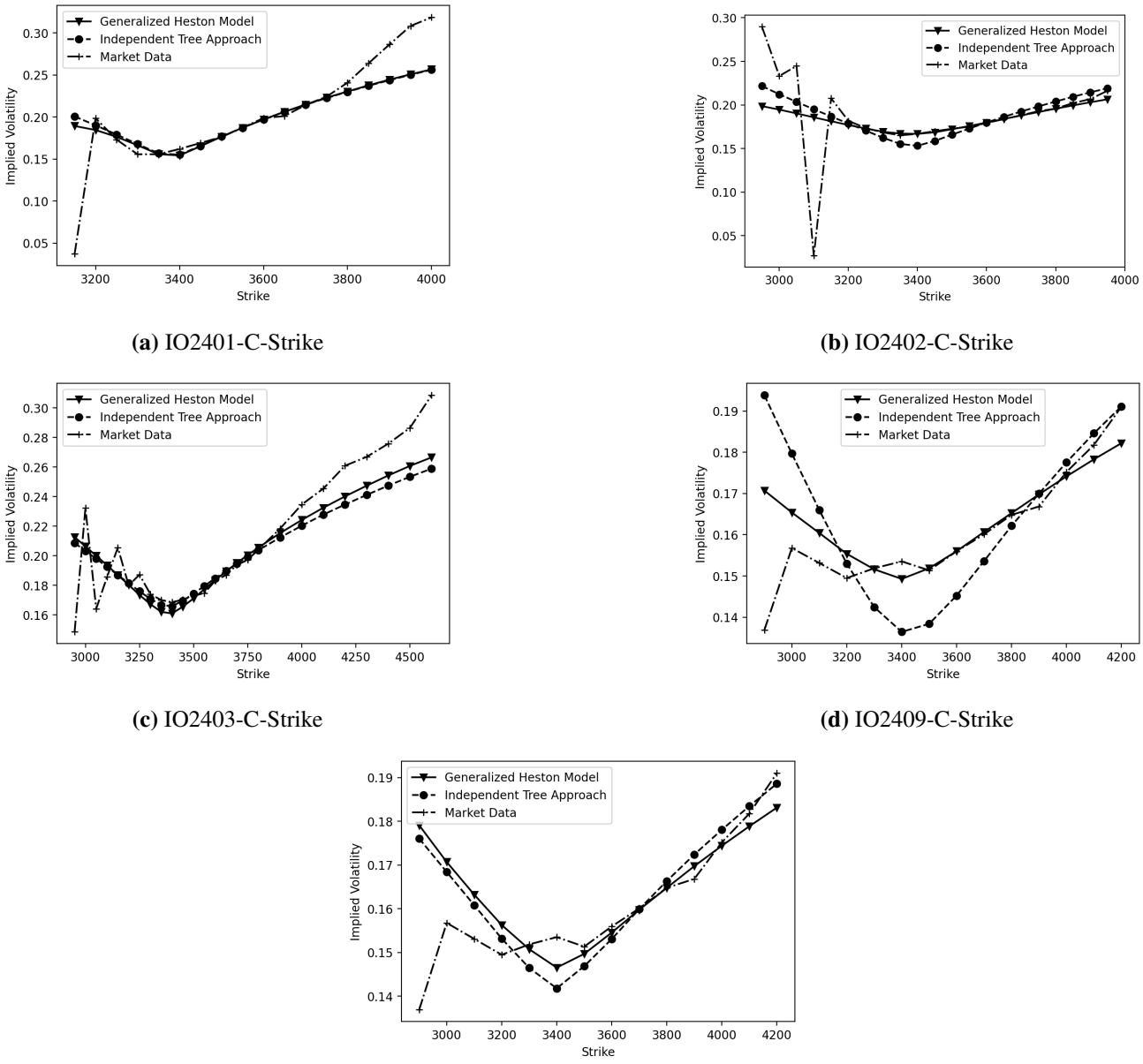

(a) IO2401-C-Strike

(b) IO2402-C-Strike

(c) IO2403-C-Strike

(d) IO2409-C-Strike

(e) IO2412-C-Strike

Figure 15. Implied volatility of CSI300 Index call options with different maturity on January 3, 2024.

Table 5. Comparison of the mean absolute error of two models.

Contract	Independent Heston tree	Correlated Heston tree	Year to maturity
IO2401-C-Strike	2.285×10^{-2}	2.217×10^{-2}	0.0465
IO2402-C-Strike	1.969×10^{-2}	1.895×10^{-2}	0.1233
IO2403-C-Strike	1.485×10^{-2}	1.395×10^{-2}	0.2000
IO2409-C-Strike	1.171×10^{-2}	5.566×10^{-3}	0.7178
IO2412-C-Strike	7.210×10^{-3}	7.071×10^{-3}	0.9671

6. Conclusion

This study extends the original two-dimensional binomial tree model to incorporate correlation between asset and volatility processes. The validation of the model's effectiveness in capturing the dynamics of the volatility process, particularly the asset process assumed in the Heston model, underscores its robustness.

The experiment involved several key analyses. First, a comparison of the variance distribution at specific time points between the tree approach and Monte Carlo simulations was conducted. The results validated the tree approach as a viable method for modeling the variance process. Second, the convergence of the two-dimensional binomial tree was tested and confirmed, demonstrating the model's reliability. Third, the error analysis of the model at zero correlation was tested, demonstrating that the generalization does not introduce significant modeling errors compared to the previous approach.

Additionally, empirical evidence from the Chinese options market was provided to further solidify the model's applicability. The refined tree model, incorporating the correlation term, offers a deterministic method for valuing European options, American options, and certain types of exotic options, thus providing a numerical approach to completing the Heston model. This deterministic nature enhances the practical utility of the model in financial markets, offering a robust and accurate tool for option pricing and risk management.

Author contributions

Conceptualization: Kow P.E., Koh Y.B., NG K.H., Yang H.
Data curation: Kow P.E.
Formal analysis: Kow P.E.
Funding acquisition: NG K.H., Yang H.
Investigation: Kow P.E.
Methodology: Kow P.E.
Software: Kow P.E.
Supervision: Koh Y.B., NG K.H.
Validation: Kow P.E., Koh Y.B., NG K.H., Yang H.
Visualization: Kow P.E.
Writing – original draft: Kow P.E.
Writing – review & editing: Kow P.E., Koh Y.B., NG K.H., Yang H.

Acknowledgments

This work was supported by the Ministry of Higher Education (MOHE), Malaysia under the Fundamental Research Grant Scheme (FRGS) with reference code: FRGS/1/2023/STG06/UM/02/1 (project no.: FP067-2023) and the National Natural Science Foundation of China (Grant No. 12471452).

Conflict of interest

Hailiang Yang is an editorial board member/guest editor for Journal of Industrial and Management Optimization and was not involved in the editorial review or the decision to publish this article.

The authors declare that there are no conflicts of interest regarding the publication of this paper.

References

1. F. Black, M. Scholes, The pricing of options and corporate liabilities, *J. Political Econ.,* **81** (1973), 637–654. https://doi.org/10.1086/260062
2. E. Derman, M. B. Miller, *The Volatility Smile*, John Wiley & Sons, 2016. https://doi.org/10.1002/9781119289258
3. E. Derman, I. Kani, The volatility smile and its implied tree, *Goldman Sachs Quantitative Strategies Research Notes,* **2** (1994), 45–60.
4. B. Dupire, Pricing with a smile, *Risk,* **7** (1994), 18–20.
5. S. L. Heston, A closed-form solution for options with stochastic volatility with applications to bond and currency options, *Rev. Financ. Stud.,* **6** (1993), 327–343. https://doi.org/10.1093/rfs/6.2.327
6. W. F. Sharpe, *Investments*, Prentice-Hall, 1978.
7. J. C. Cox, S. A. Ross, M. Rubinstein, Option pricing: A simplified approach, *J. Financ. Econ.,* **7** (1979), 229–263. https://doi.org/10.1016/0304-405X(79)90015-1
8. J. A. Pareja-Vasseur, F. H. Marín-Sánchez, Quadrinomial trees to value options in stochastic volatility models, *J. Deriv.,* **27** (2019), 49–66. https://doi.org/10.3905/jod.2019.1.076
9. X. Y. Wu, C. Q. Ma, S. Y. Wang, Warrant pricing under GARCH diffusion model, *Econ. Model.,* **29** (2012), 2237–2244. https://doi.org/10.1016/j.econmod.2012.06.020
10. U. H. Lok, Y. D. Lyuu, A valid and efficient trinomial tree for general local-volatility models, *Comput. Econ.,* **60** (2022), 817–832. https://doi.org/10.1007/s10614-021-10166-x
11. S. K. Nawalkha, N. A. Beliaeva, Efficient trees for CIR and CEV short rate models, *J. Altern. Invest.,* **10** (2007), 71–90. https://doi.org/10.3905/jai.2007.688995
12. N. A. Beliaeva, S. K. Nawalkha, A simple approach to pricing American options under the Heston stochastic volatility model, *J. Deriv.,* **17** (2010), 25. https://doi.org/10.3905/jod.2010.17.4.025
13. D. B. Nelson, K. Ramaswamy, Simple binomial processes as diffusion approximations in financial models, *Rev. Financ. Stud.,* **3** (1990), 393–430. https://doi.org/10.1093/rfs/3.3.393
14. Y. D. Lyuu, *Financial Engineering and Computation: Principles, Mathematics, Algorithms*, Cambridge University Press, 2002.
15. W. H. Fleming, H. M. Soner, *Controlled Markov Processes and Viscosity Solutions*, Springer, 2006, 321–346. https://doi.org/10.1007/0-387-31071-1
16. J. C. Cox, J. E. Ingersoll, S. A. Ross, A theory of the term structure of interest rates, *Econometrica,* **53** (1985), 385–407. https://doi.org/10.2307/1911242
17. J. Hull, A. White, Numerical procedures for implementing term structure models I: Single-factor models, *J. Deriv.,* **2** (1994), 7–16. https://doi.org/10.3905/jod.1994.407902

18. M. Mrázek, J. Pospíšil, Calibration and simulation of Heston model, *Open Math.,* **15** (2017), 679–704. https://doi.org/10.1515/math-2017-0058

19. A. Ortiz-Ramírez, F. Venegas-Martínez, M. T. V. Martínez-Palacios, Parameter calibration of stochastic volatility Heston's model: Constrained optimization vs. differential evolution, *Contaduría y Administración,* **67** (2022). https://doi.org/10.22201/fca.24488410e.2022.2789

20. Y. Cui, S. del Baño Rollin, G. Germano, Full and fast calibration of the Heston stochastic volatility model, *Eur. J. Oper. Res.,* **263** (2017), 625–638. https://doi.org/10.1016/j.ejor.2017.05.018

21. F. A. Longstaff, E. S. Schwartz, Valuing American options by simulation: A simple least-squares approach, *Rev. Financ. Stud.,* **14** (2001), 113–147. https://doi.org/10.1093/rfs/14.1.113

22. A. A. Christie, The stochastic behavior of common stock variances: Value, leverage and interest rate effects, *J. Financ. Econ.,* **10** (1982), 407–432. https://doi.org/10.1016/0304-405X(82)90018-6

AIMS Press